SoftwareX 30 (2025) 102099

Contents lists available at ScienceDirect

SoftwareX

journal homepage: www.elsevier.com/locate/softx

CryoEvap: An open-source software to simulate the evaporation of cryogenic liquids in vertically orientated storage tanks

Felipe Huerta [a,*], Velisa Vesovic [b]

[a] Department of Chemical and Bioprocess Engineering, Pontificia Universidad Católica de Chile, Santiago, Chile
[b] Department of Earth Science and Engineering, Imperial College London, London, SW7 2AZ, United Kingdom

ARTICLE INFO

Keywords:
Hydrogen
Cryogenics
Evaporation
BOG
Energy storage

ABSTRACT

The paper presents a new software tool, CryoEvap, based on a novel and validated modelling approach that simulates the isobaric evaporation of cryogenic liquids in storage tanks. CryoEvap provides time-dependent liquid volume, boil-off gas rates, boil-off gas temperature, average vapour temperature, vapour temperature profiles, different heat ingresses and estimates of transient time relevant to industrial applications in cryogenic energy storage. The software has been implemented in Python under an object-oriented programming paradigm. CryoEvap is designed to aid research in novel applications such as renewable energy storage and the optimal integration of the storage tanks into process simulators. In this paper we provide new research insights into the behaviour of cryogens when stored in two industry-relevant scenarios of large and medium scale storage. The results indicate that the transient period varies drastically between different sized storage tanks and that the inclusion of the vapour thermal expansion is an essential pre-requisite for good estimates of the boil-off gas rates.

1. Metadata

Nr	Code metadata description	*Metadata*
C1	Current code version	v1.0
C2	Permanent link to code/repository used for this code version	https://github.com/felipehuerta17/CryoEvap-v1
C3	Permanent link to reproducible capsule	
C4	Legal code license	GNU General Public License version 3 (GPL 3.0)
C5	Code versioning system used	Git
C6	Software code languages, tools and services used	Python
C7	Compilation requirements, operating environments and dependencies	Python 3.9, scipy 1.9.1, matplotlib 3.5.2, coolprop 6.4.3, numpy 2.0.2
C8	If available, link to developer documentation/manual	https://github.com/felipehuerta17/CryoEvap-v1/blob/main/README.md
C9	Support email for questions	fnhuerta@uc.cl

2. Motivation and significance

Cryogenic liquids are substances with a boiling point below −150 °C. They are widely used in refrigeration, manufacturing [1], and in several energy storage technologies that make use of liquefied natural gas (LNG) [2], liquid hydrogen (LH_2) [3] or liquid air [4]. These liquids are stored in insulated tanks subject to heat ingress from the surroundings [5], which leads to cryogen evaporation and pressure build-up [6]. Once the tank reaches the maximum allowable working pressure, the evaporated cryogen, known as boil-off gas (BOG), must be removed. For mid and large-scale storage, the operating pressure is slightly above atmospheric, which results in an approximately isobaric BOG removal [7]. In most industrial applications, BOG is captured and re-liquefied, although strategies also include flaring at regasification terminals, reutilising the BOG as fuel during shipping [8] or venting for safety in extreme cases. For all these BOG management strategies, minimising BOG is pivotal, as it decreases economic and environmental costs and improves process safety.

To minimise BOG, engineers use cryogen evaporation models ranging from simple bulk-parameter models to complex multiphase computational fluid dynamics (CFD) simulations. The simplest models often fail to capture vapour phase heat transfer, natural convection, and thermal expansion that govern BOG generation [7]. While complex CFD models are accurate, they rely on difficult-to-measure parameters and are computationally costly, limiting their use in optimization and

* Corresponding author.
E-mail address: fnhuerta@uc.cl (F. Huerta).

https://doi.org/10.1016/j.softx.2025.102099
Received 8 December 2024; Received in revised form 12 February 2025; Accepted 13 February 2025
Available online 20 February 2025

practical applications.

This work presents `CryoEvap`, an open-source Python module for simulating isobaric evaporation of cryogenic liquids developed using an object-oriented programming (OOP) paradigm. It achieves a good compromise between accuracy, complexity and practicality, enabling easy simulation of storage tanks to quantify BOG rates, liquid volume and vapour temperatures during the isobaric storage. The governing equations of the physical model are based on the well-established Huerta and Vesovic isobaric evaporation model [7], validated through experiments [9,10] and CFD simulations [11]. Two novel modifications have been made to enhance model accuracy: (i) a wall heat partitioning factor has been introduced to allow for a more accurate description of the distribution of external heat between liquid and vapour phases [10] and (ii) thermophysical properties are calculated using a Helmholtz-energy-based equation of state [12].

3. Software description

3.1. Software architecture

`CryoEvap` was developed using an object-oriented approach to distinguish the cryogenic liquid from the storage tank. The mass and energy balances that govern the evolution of the cryogen mass, volume and enthalpy are functions of the tank geometry and its heat transfer properties. The Tank class defines tank properties and includes simulation control attributes and functions. Each Tank includes a `Cryogen` instance, which contains thermophysical properties and functions for spatial averages relevant to macroscopic balances. The `Plots` class visualises BOG rates, liquid volume, heat transfer rates and vapour temperature profiles. Fig. 1 shows a unified modelling language (UML) diagram of `CryoEvap` created using GenMyModel.

3.2. Software functionality

3.2.1. Tank class

The `Tank` class represents a vertical cylindrical storage tank with a constructor that takes internal diameter, external diameter, volume, and initial filling as inputs to calculate cross-sectional area and height. This class include simulation parameters such as the dimensionless grid `z_grid` for the vapour phase discretisation, and the `sol` dictionary for storing results. Its member functions are organized into properties, ODE implementations, and utilities. The properties that are updated at each time-step include vapour height, wall areas in contact with liquid and vapor, heat ingress, advective velocity [7] and the evaporation rate. `CryoEvap` uniquely provides quick estimates of the initial evaporation rate and transient period through the `b_l_dot` and `tau` properties, enabling rapid assessment without requiring a full simulation, see Fig. 1.

The tank heat transfer properties are set using the `set_HeatTransProps` function. This function requires the following input parameters: (i) the temperature of the surroundings; (ii) the overall heat transfer coefficients for the liquid and vapour phases and (iii) the wall heat partitioning fraction, `eta_w`. This value is defined as the fraction of the external vapour heat ingress that is conducted downwards through the dry wall to the vapour-liquid interface [10]. The optional input parameters are the bottom and roof heat ingresses. If unspecified, they are calculated using the liquid and vapour overall heat transfer coefficients and the temperature difference at the tank bottom and roof, respectively [7].

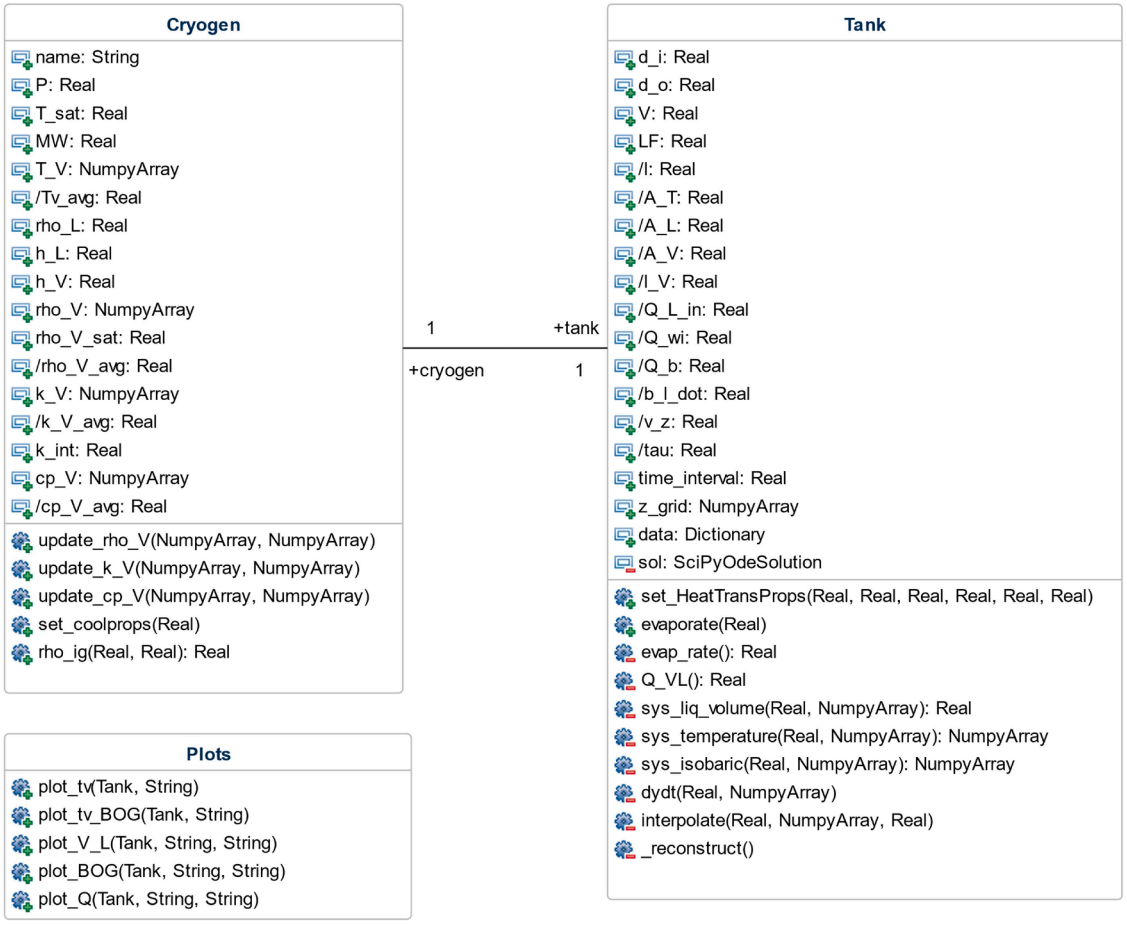

Fig. 1. Unified modelling language (UML) diagram of `CryoEvap`.

The `Tank` class includes an empty instance of the `Cryogen` class. This attribute must be set with an initialised `Cryogen` object to run the simulation. The simulation can be executed via the `evaporate` function after constructing the `Tank` and setting its heat transfer and cryogen attributes. This function takes the simulation time as a parameter and applies Huerta and Vesovic's isobaric evaporation model [7], adjusted for wall heat partitioning [10]. Simulation results are stored in the `Tank` object's `data` dictionary attribute. The numerical methods used to solve the system of ordinary differential equations are detailed in Subsection 3.2.4.

3.2.2. Cryogen class

The `Cryogen` class calculates the thermophysical properties of cryogens in liquid and vapour phases using the COOLPROP [12] library. Its constructor takes a cryogen name consistent with COOLPROP's [12] definitions. The `set_coolprops` function calculates these properties, assuming initial liquid and vapour temperatures equal to the saturation temperature at a given operating pressure. As evaporation progresses, vapour temperature and its properties, such as density, thermal conductivity, and heat capacity, vary. These properties are updated at each time step through the `update_rho_V`, `update_k_V` and `update_cp_V` functions.

3.2.3. Plots class

The `Plots` class enables the visualization of quantities of engineering interest frequently used in cryogen evaporation research [7,9,13–15]. Functions can only be called after a simulation concludes and results are stored in the `sol` object. The `plot_tv` function displays the vapour temperature profile over dimensionless length at six timesteps. If the fully dimensional vapour temperature is required, the attribute `z_grid` must be multiplied by the vapour height. The vapour height can be obtained by subtracting the interface position from the tank height attribute, `l`. The interface position can be obtained by dividing the liquid volume stored in the V_L column of the `data` dictionary, by the tank transverse area defined as the `A_T` attribute of the storage tank.

The `plot_Q` function creates a 2×2 subplot displaying heat transfer rates over time, including liquid and vapour heating, vapour to liquid and wall-to-interface heat transfers. The `plot_V_L` and `plot_BOG` functions create plots of liquid volume and boil-off gas rates as a function of time, respectively, while `plot_tv_BOG` displays average vapour and boil-off gas temperatures as a function of time.

3.2.4. Numerical methods

The numerical method follows the approach in the Huerta and Vesovic model [7], using a system of differential equations consisting of an ordinary differential equation (ODE) for liquid volume and a partial differential equation (PDE) for the vapour phase. The system of equations solved by `CryoEvap` can be found in Supplementary Material SM1. The PDE is spatially discretised using the method of lines [16] and the finite difference method, resulting in an ODE system where each equation represents the temperature at a node. The first and second spatial derivatives of vapour temperature were discretised using second-order accurate central differences. A Dirichlet boundary condition of constant temperature is used at the vapour-liquid interface, while second-order backward differences are applied at the tank roof. Neumann and Robin boundary conditions are implemented for fixed heat flux and natural convection heating, respectively. A grid spacing of $\Delta z = 0.1$ m was selected for all scenarios as it was sufficient to achieve grid independence. The ODE system that represents the model is processed with NumPy and solved using the SciPy's solve_ivp function. Explicit algorithms based on the Runge-Kutta method proved more stable and accurate than implicit algorithms. Therefore, the method argument in solve_ivp was set to RK45, which provided the best accuracy, with both absolute and relative tolerances set to 10^{-6}. Simulations took between 20 and 150 s on a single core of an Intel® i7–11800H 4.2 GHz processor.

4. Illustrative examples

Two scenarios relevant to the industry for different cryogens and scales are presented to illustrate: (i) new physical insight obtained using `CryoEvap` and (ii) its capability to improve the description of the isobaric evaporation process. The full implementation is available in the `CryoEvap` repository. A brief user guide with installation instructions can be found in Supplementary Material SM2. The cryogen name, tank geometry, initial liquid filling, operating pressure and the heat transfer parameters can be found in Supplementary Material SM3.

4.1. Medium-scale liquid hydrogen storage

The first scenario consists of the isobaric evaporation of LH_2 in a medium-scale 2033 m^3 vertically orientated cylindrical storage tank. The tank properties and operating conditions were obtained from NASA's Space Launch System for the Artemis program [17]. The overall heat transfer coefficients were fitted, assuming a boil-off rate (BOR) of 0.29 %. The wall heat partitioning was set to $\eta_w = 0.8$ considering a representative vapour superheating of 4 K of a smaller scale NASA LH_2 vertically orientated storage tank [18]. The initial liquid filling was set to 50 %. Fig. 2 shows the vapour temperature profile for this scenario, where the vertical coordinate represents the dimensionless distance from the vapour-liquid interface, and the abscissa is the temperature. The temperature increases monotonically with time and vapour height. Six different timesteps are depicted in colours of increasing brightness, from dark grey at the beginning of the evaporation to yellow at the end of the transient period, $\tau = 314$ h. At an early stage of evaporation ($t = 52$ h), the vapour temperature remains spatially homogeneous far from the vapour liquid interface ($\zeta > 0.4$). Near the vapour-liquid interface, $\zeta < 0.4$, a sharp temperature gradient is observed. The temperature profile develops with time from the interface towards the tank roof until a pseudo-steady state is reached. At this time, depicted in a yellow line in Fig. 2, the maximum vapour superheating with respect to the interface is 4.6 K. The linear shape of the pseudo-steady state temperature profile implies that advection heat transfer dominates over wall heating [19]. During the simulation period, the interface was displaced downwards owing to evaporation from 20.22 m to 19.46 m. This resulted in an increase of 3.7 % of the vapour height, which should be taken into consideration if it is required to reconstruct the fully dimensional vapour temperature profile.

Fig. 3 shows the heat ingresses obtained with the function `plot_Q`. Fig. 3a shows the external vapour heat ingress ($\dot{Q}_{V,ext}$) as a blue line and the wall-to-interface heat ingress ($\dot{Q}_{V,w}$) as a yellow line. It demonstrates that both increase monotonically with time, as a consequence of the increase in the vapour-wall area with the progress of evaporation. Fig. 3b shows the evolution of the total heat ingress into the liquid, $\dot{Q}_{tot} = \dot{Q}_b + \dot{Q}_L + \dot{Q}_{VL} + \dot{Q}_{V,w}$, which after initial 60 min decreases monotonically. In addition to $\dot{Q}_{V,w}$, the total heat ingress is the sum of the liquid heat ingress through the walls, $\dot{Q}_L$, the vapour to liquid heat ingress, $\dot{Q}_{VL}$, and the heat ingress through the bottom, $\dot{Q}_b$. It is interesting to observe that the total heat ingress barely changes through the transient period (0.8 %), as the decrease of heat ingress through the walls in contact with a liquid, $\dot{Q}_L$, is balanced by the increase in the wall-to-interface heat ingress, $\dot{Q}_{V,w}$.

Fig. 4 shows the evaporation and BOG rates obtained with the function `plot_BOG`. The evaporation rate decreases monotonically with time as it is directly proportional to the total heat ingress, see Fig. 3b. Fig. 4 also shows that the BOG rate decreases monotonically, but at a much higher rate initially. The initial rapid decrease is driven by the vapour thermal expansion [7] and corresponding decrease in vapour density. For hydrogen at very low temperatures, the rate of change of vapour density with respect to temperature is pronounced. After 165 h, the BOG rate is slightly lower than the evaporation rate because a small

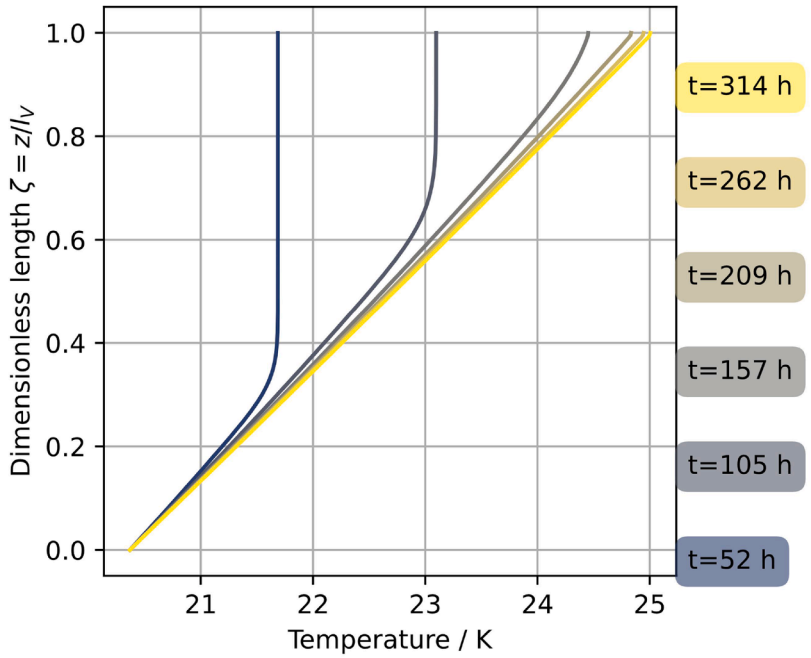

Fig. 2. Vapour temperature profile for the isobaric evaporation of LH_2 in a 2033 m^3 storage tank filled to 50 % of its capacity.

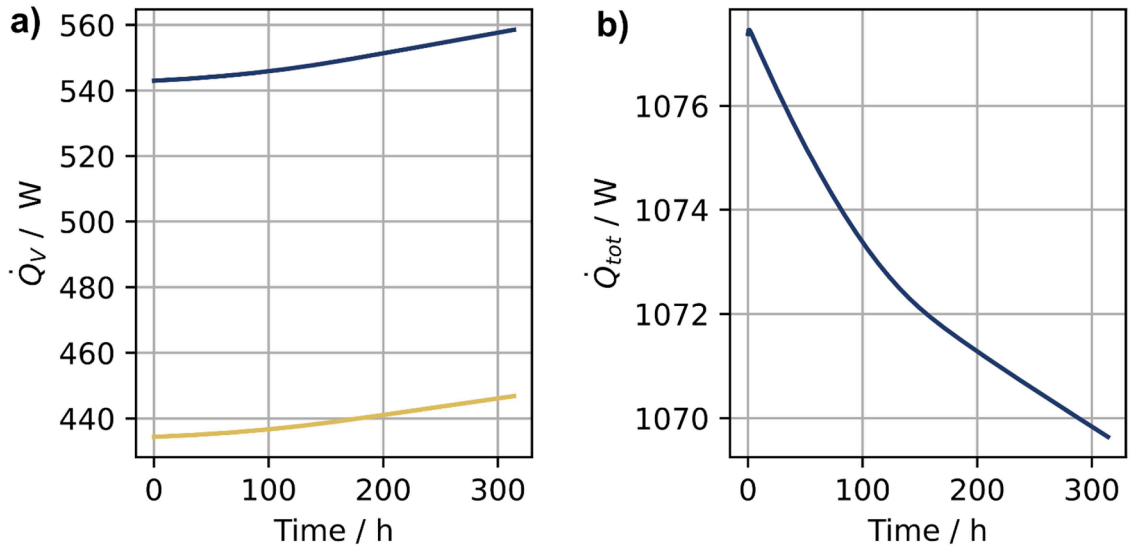

Fig. 3. Heat ingresses during the isobaric evaporation of LH_2 in a 2033 m^3 storage tank filled to 50 % of its capacity.

fraction of the evaporated cryogen accumulates in the tank as the liquid volume decreases [7].

4.2. Large scale methane storage

Scenario 2 consists of liquid methane (LCH_4) storage in a 165,000 m^3 tank commonly used in LNG receiving terminals. The tank geometry was obtained from Migliore et al. [5] based on the standard LNG storage tank used in the industry. The model parameters were fitted once the temperature pseudo-steady state was reached. An initial liquid filling of 55 % was selected, displaying an average vapour temperature 32 K higher than the methane saturation temperature at 116.3 kPa and a boil-off rate of 0.15 %. These values of vapour superheating and boil-off rates are commonly observed in industrial operations. The fitting resulted in a wall heat partitioning coefficient of $\eta_w = 0.70$ and overall heat transfer coefficients $U_L = U_V = 0.19\ W\ m^{-2}\ K^{-1}$. A 48-week simulation period was selected to observe long-term dynamics.

The vapour temperature profiles are similar to those observed for Scenario 1, see Fig. 2. The transient period is $\tau = 130$ h and the maximum vapour superheating at the end of the transient period is 35 K. Following the transient period, a linear temperature profile is established in the vapour phase with the temperature at the top of the tank and consequently the BOG temperature, increasing monotonically with time, reaching 172 K after 48 weeks. The vapour superheating is smaller than that observed in Huerta and Vesovic original model [7], as that model did not account for the wall heat partitioning coefficient. During the simulation, the interface was displaced downwards due to evaporation from 19.80 m to 10.71 m. This represents a 56 % increase in the vapour height, an order of magnitude larger than that of Scenario 1, owing to the longer evaporation period in Scenario 2.

Fig. 5 shows the heat ingresses for Scenario 2. In contrast to the medium-scale storage of LH_2, Fig. 5a illustrates that both external

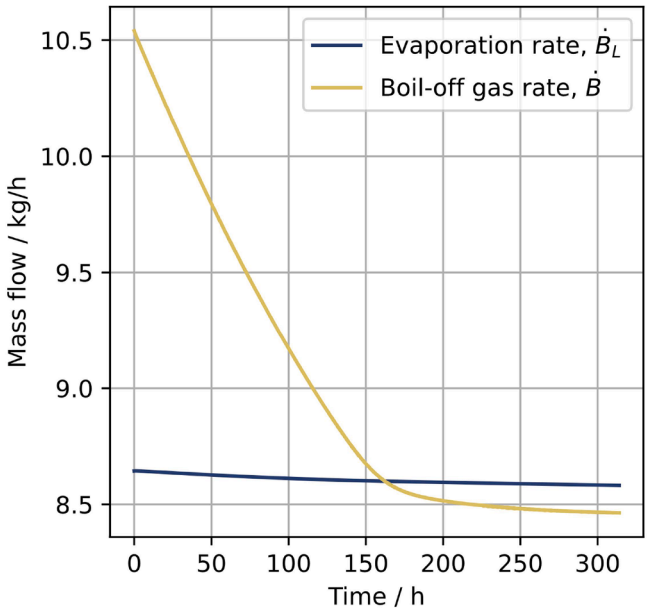

Fig. 4. Evaporation and BOG rates for the isobaric evaporation of LH_2 in a 2033 m^3 storage tank filled to 50 % of its capacity.

vapour and wall-to-interface heat ingresses first decrease sharply during the first 90 h of evaporation and then increase slowly with time. The local minimum is a consequence of the 20 % reduction in temperature driving force, $T_{air} - \overline{T}_V$, owing to vapour heating, and the subsequent increase of vapour area in contact with the walls [7,11]. Fig. 5b shows that the total liquid heat ingress decreases sharply during the transient period, followed by a slower decrease during the remaining 47 weeks. Overall, the total heat ingress into the liquid decreased by 2.1 % during the transient period compared to 0.7 % for Scenario 1, although the transient period was 2.4 times longer in Scenario 1. This is a consequence of the rapid decrease in wall-to-interface heat ingress, see Fig. 5a, observed for Scenario 2 but not for Scenario 1.

Fig. 6 illustrates that the evaporation rate initially decreases rapidly and then more slowly, following the trend of the total liquid heat ingress, see Fig. 5b. The BOG rate decreases sharply from 3023.5 to 2297 kg/h during the transient period and then slowly to 2010 kg/h at the end of the 48 weeks. The BOG rate intersected the evaporation rate after 94 h, corresponding to 72.3 % of the transient period, compared to 52.5 % for Scenario 1.

The two scenarios illustrate that medium and large-scale storage of cryogen display a number of different physical characteristics that must be properly accounted for. In particular, the qualitatively different behaviour of the total liquid ingress during the transient period and the difference in the magnitude of the vapour superheating which governs the BOG temperature. After the pseudo-steady state is achieved, the ratio between the BOG rate, $\dot{B}$, and the evaporation rate, $\dot{B}_L$, depends on the ratio of the densities between the cryogen and its vapour as $\dot{B} = \dot{B}_L(1 - \rho_V/\rho_L)$ [5]. For liquid hydrogen, $\rho_V/\rho_L \approx 0.019$ while for liquid methane this quantity is 0.006. This explains the smaller differences between BOG and evaporation rates for liquid methane, see Fig. 6, than for liquid hydrogen, see Fig. 4.

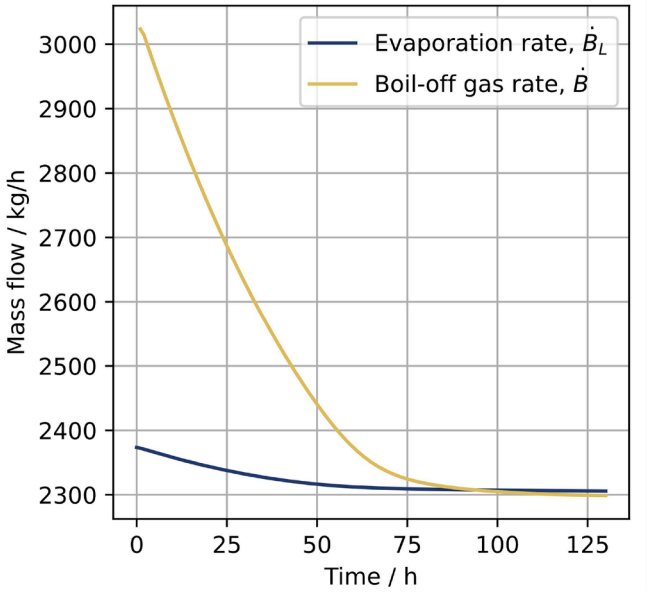

Fig. 6. Evaporation and BOG rates for the isobaric evaporation of methane in a 165,000 m^3 storage tank filled to 55 % of its capacity.

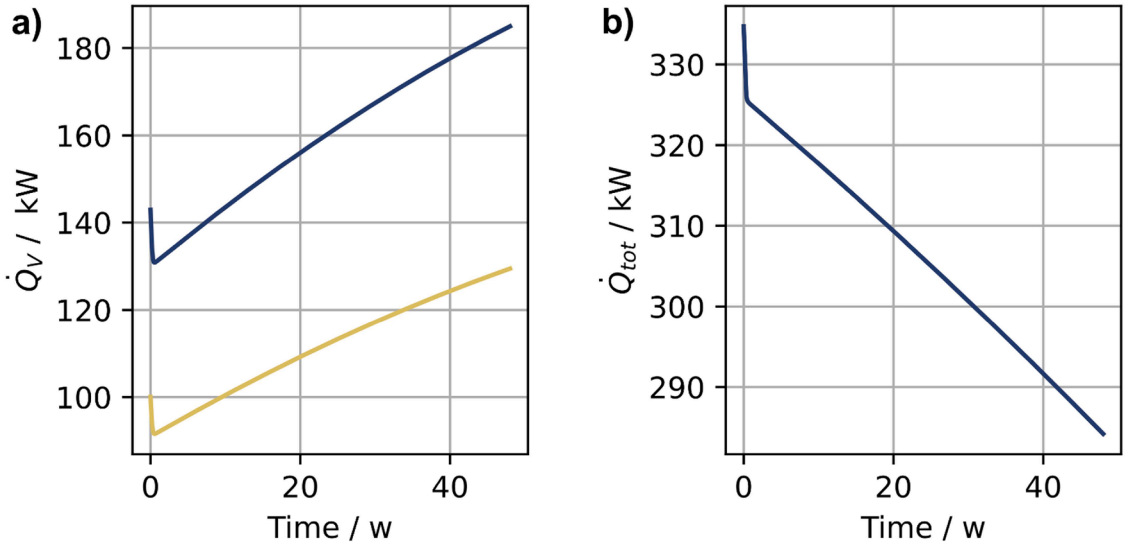

Fig. 5. Heat ingresses during the isobaric evaporation of methane in a in a 165,000 m^3 storage tank filled to 55 % of its capacity.

5. Impact

CryoEvap provides a more accurate alternative to traditional lumped mass and energy balance models for cryogen isobaric evaporation [5,20–22]. It simulates the evaporation seven orders of magnitude faster than CFD models [11,23–25], hastening parametric studies and sensitivity analyses. CryoEvap can be integrated easily with process simulation software, and the sub-models are straightforward to modify. This will help researchers and industrial users optimise cryogen storage. For instance, BOG minimisation as a function of different liquid fillings or storage tank aspect ratios, at the design level, can be performed in less than two hours of computation time. We specifically foresee CryoEvap to play a significant role in developing optimal and integrated solutions for liquid hydrogen storage. Furthermore, while large-scale experimental data in the public domain remain scarce, the open-source nature of CryoEvap enables users to calibrate the model with their own experimental data, thereby mitigating risks when extending its application to large industrial systems.

The primary, widely available, free software for the simulation of the evaporation of cryogenic liquids is currently BoilFAST [26]. BoilFAST offers a user-friendly interface, allowing engineers to simulate both isobaric and non-isobaric evaporation scenarios for cryogens such as LNG [22] and LH2 [27] in different tank geometries. However, BoilFAST's underlying model relies on bulk-phase approximations that model the interface heat transfer using a single empirical heat transfer coefficient. Thus, only estimates of boil-off rates and average vapour temperatures are provided. Unlike BoilFAST, CryoEvap provides detailed spatial-temporal vapour temperature profiles, including BOG temperature and an estimate of the transient time. The latter provides the user with a measure of the onset of the pseudo-steady state. Furthermore, the variable timestep used by CryoEvap makes it more suitable for analysing long-term cryogen storage.

6. Conclusions

CryoEvap simulates the isobaric evaporation of cryogenic liquids in vertically oriented storage tanks. The underlying model achieves a balance between accuracy and complexity. It enhances our previous model [7], improving the accuracy of thermophysical properties calculation and vapour heat ingress modelling. CryoEvap provides time evolution data for BOG rate and temperature, spatial vapour temperature profiles, heat ingress rates, and pseudo-steady state onset. It delivers granular data for in-depth analysis with more accuracy than mainstream process simulators. In particular, it provides the spatio-temporal vapour temperature profile, a unique feature of CryoEvap that is used to calculate other quantities. The software has been demonstrated through two industry-relevant scenarios, emphasizing the significance of accounting for the transient period at the beginning of the evaporation. Notably, the BOG temperature can exceed the average vapour temperature by more than >30 K in long-term storage, and initial BOG rates are usually higher than evaporation rates due to thermal expansion. CryoEvap is designed in Python using an OOP approach to improve the BOG management of cryogen storage units and the accuracy of techno-economic analyses of LNG, liquid hydrogen and liquid air energy storage plants. It is easily customizable for other applications relevant to the industry, such as cryogen loading and unloading.

CRediT authorship contribution statement

Felipe Huerta: Writing – review & editing, Writing – original draft, Software, Methodology, Investigation, Formal analysis, Conceptualization. **Velisa Vesovic:** Writing – review & editing, Writing – original draft, Formal analysis, Conceptualization.

Declaration of competing interest

The authors declare that they have no known competing financial interests or personal relationships that could have appeared to influence the work reported in this paper.

Acknowledgments

F. Huerta appreciates the financial support by the project ANID FONDECYT DE INICIACION FOLIO 11241050 of the National Agency of Research and Development (ANID), Chile, and the project ANID/FONDAP /1523A0006 'Solar Energy Research Centre' - SERC - Chile.

Supplementary materials

Supplementary material associated with this article can be found, in the online version, at doi:10.1016/j.softx.2025.102099.

References

[1] Yildiz Y, Nalbant M. A review of cryogenic cooling in machining processes. Int J Mach Tools Manuf 2008;48:947–64.
[2] Liu Y, Guo K. A novel cryogenic power cycle for LNG cold energy recovery. Energy 2011;36:2828–33.
[3] Andersson J, Grönkvist S. Large-scale storage of hydrogen. Int J Hydrogen Energy 2019;44:11901–19.
[4] Park JH, Kim N, Lee JI. The effect of insulation on boil-off gas in liquid air storage tank. Energy 2024;291:130265.
[5] Migliore C, Tubilleja C, Vesovic V. Weathering prediction model for stored liquefied natural gas (LNG). J Nat Gas Sci Eng 2015;26:570–80.
[6] Schmidt AF, Purcell JR, Wilson WA, Smith RV. An experimental study concerning the pressurization and stratification of liquid hydrogen. J Res Natl Bur Stand 1960: 487–97.
[7] Huerta F, Vesovic V. A realistic vapour phase heat transfer model for the weathering of LNG stored in large tanks. Energy 2019;174:280–91.
[8] Al-Sobhi SA, AlNouss A, Shamlooh M, Al-Nuaimi K, AlMulla A, Khraisheh M. Sustainable boil-off gas utilization in liquefied natural gas production: economic and environmental benefits. J Clean Prod 2021;296:126563.
[9] Seo M, Jeong S. Analysis of self-pressurization phenomenon of cryogenic fluid storage tank with thermal diffusion model. Cryogenics 2010;50:549–55.
[10] Huerta F, Vesovic V. CFD modelling of the non-isobaric evaporation of cryogenic liquids in storage tanks. Appl Energy 2024;356:122420.
[11] Huerta F, Vesovic V. CFD modelling of the isobaric evaporation of cryogenic liquids in storage tanks. Int J Heat Mass Transf 2021;176:121419.
[12] Bell IH, Wronski J, Quoilin S, Lemort V. Pure and pseudo-pure fluid thermophysical property evaluation and the open-source thermophysical property library CoolProp. Ind Eng Chem Res 2014;53:2498–508.
[13] Kang M, Kim J, You H, Chang D. Experimental investigation of thermal stratification in cryogenic tanks. Exp Therm Fluid Sci 2018;96:371–82.
[14] Perez F, Al Ghafri SZS, Gallagher L, Siahvashi A, Ryu Y, Kim S, et al. Measurements of boil-off gas and stratification in cryogenic liquid nitrogen with implications for the storage and transport of liquefied natural gas. Energy 2021;222:119853.
[15] Al Ghafri SZS, Perez F, Heum Park K, Gallagher L, Warr L, Stroda A, et al. Advanced boil-off gas studies for liquefied natural gas. Appl Therm Eng 2021;189:116735.
[16] Schiesser WE, Griffiths GW. A compendium of partial differential equation models: method of lines analysis with matlab. 1st ed. Cambridge; New York: Cambridge University Press; 2009.
[17] Fesmire J, Swanger A. Overview of the new LH2 sphere at NASA Kennedy space center. U. S. Department of Energy National Aeronautics Space Administration; 2021.
[18] Hastings LJ, Flachbart RH, Martin JJ, Hedayat A, Fazah M, Lak T, et al. Spray bar zero-gravity vent system for on-orbit liquid hydrogen storage. U. S. Department of Energy National Aeronautics Space Administration; 2003.
[19] Huerta F, Vesovic V. Analytical solutions for the isobaric evaporation of pure cryogens in storage tanks. Int J Heat Mass Transf 2019;143:118536.
[20] Miana M, Del Hoyo R, Rodrigálvarez V. Comparison of evaporation rate and heat flow models for prediction of liquefied natural Gas (LNG) ageing during ship transportation. Fuel 2016;177:87–106.
[21] Pellegrini LA, Moioli S, Brignoli F, Bellini C. LNG technology: the weathering in above-ground storage tanks. Ind Eng Chem Res 2014;53:3931–7.
[22] Al Ghafri SZS, Swanger A, Park KH, Jusko V, Ryu Y, Kim S, et al. Advanced boil-off gas studies of liquefied natural gas used for the space and energy industries. Acta Astronaut 2022;190:444–54.
[23] Jeon G-M, Park J-C, Choi S. Multiphase-thermal simulation on BOG/BOR estimation due to phase change in cryogenic liquid storage tanks. Appl Therm Eng 2021;184:116264.
[24] Saleem A, Farooq S, Karimi IA, Banerjee R. A CFD simulation study of boiling mechanism and BOG generation in a full-scale LNG storage tank. Comp Chem Eng 2018;115:112–20.

[25] Kassemi M, Kartuzova O, Hylton S. Validation of two-phase CFD models for propellant tank self-pressurization: crossing fluid types, scales, and gravity levels. Cryogenics 2018;89:1–15.

[26] Jusko V, Al Ghafri SZS, May EF. BoilFAST v1.1.0. Fluid Sciences and Resources Division. Perth, Australia: The University of Western Australia; 2021.

[27] Al Ghafri SZS, Swanger A, Jusko V, Siahvashi A, Perez F, Johns ML, et al. Modelling of liquid hydrogen boil-off. Energies 2022;15:1149.